Discussion of PDF aspects

Jan Kretzschmar, University of Liverpool
W mass workshop Mainz

09.02.2017

Introduction

- PDF uncertainties on m_W measurement in pp or $p\bar{p}$ typically among the leading systematics
- Typical PDF uncertainty estimates for "simple" determination at level $\pm(8-15)$ MeV depending on PDF set, with variations between different PDF sets of up to ± 20 MeV [PRD 91 (2015) 113005] – larger than precision goal
- CDF & D0 at Tevatron quoted $\pm(10-14)$ MeV
- ATLAS quoted ± 9.2 MeV [arXiv:1701.07240], exploiting (anti-)correlations between η_ℓ categories and $W^+ - W^-$ [PRD 92 (2015) 033008, EPJC (2015) 75:601]

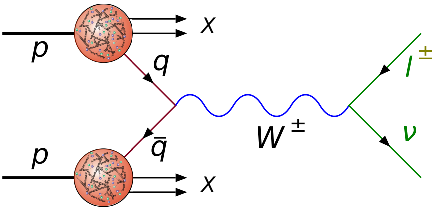

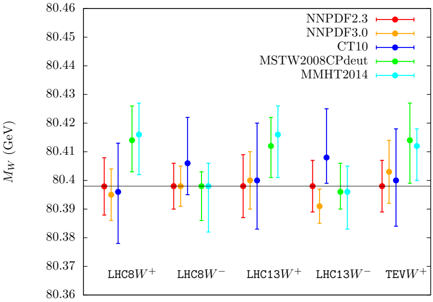

Modern PDF sets

- HERA DIS data (NC+CC) basis of all PDF sets in relevant range $x \sim 10^{-3}$–10^{-1}, not sufficient to disentangle e.g. light-quark flavours u, d, s relevant for W, Z production at LHC
- PDF sets vary in theoretical approaches and additional data sets
- W, Z cross-section data from Tevatron and/or LHC obviously important to "validate" and constrain PDFs used for m_W measurement
- Gluon at large x constrained further by jets (so far typically NLO, NNLO becoming available) and $t\bar{t}$ – less critical for m_W?
- (preliminary) updates expected/available: CT14HERA2, MMHT16, NNPDF3.1 ...

	CT14	MMHT14	NNPDF3.0	HERAPDF2.0	ABMP16	CJ12(15)	JR14
HERA data	HERA I+ charm	HERA I charm jets	HERA I+ H1 and ZEUS II charm	HERA I+II	HERA I+II charm	HERA I	HERA I charm jets
Fix. Target DIS	✓	✓	✓	✗	✓	JLAB, high x ✓	JLAB, high x ✓
Tevatron W,Z	✓	✓	✓	✗	✗/✓	✓	✗
Tevatron Jets	✓	✓	✓	✗	✗	✗	✓
Fix. Target DY	✓	✓	✓	✗	✓	✓	✓
LHC W,Z	✓	✓	✓	✗	✓	✗	✗
LHC jets	✓	✓	✓	✗	✗	✗	✗
LHC top	✗	✓	✓	✗	✓	✗	✗
LHC charm	✗	✗	✓	✗	✗/✓	✗	✗
References	arXiv:1506.07443	arXiv:1412.3989	arXiv:1410.8849	arXiv:1506.06042	arXiv:1701.05838	arXiv:1212.1702	arXiv:1403.1852

adapted from V. Radescu, QCD@LHC2016

Modern PDF sets

[J.Phys.G: Nucl.Part.Phys. 43 023001 (2016)]

$q\bar{q}$ (and flavour-composition) most relevant for W, Z production; gg less relevant directly, but correlated – differences large, can be tested with LHC data

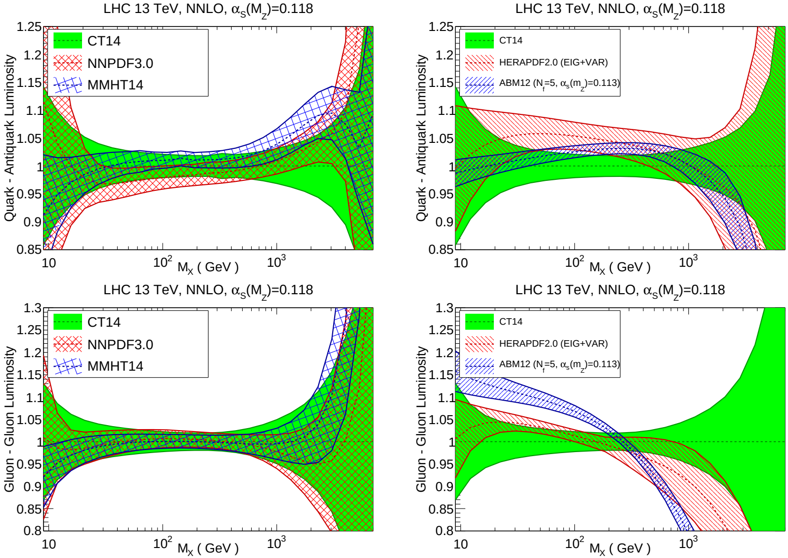

Predictions for W and Z Production

Typically different tools used for PDF fits and m_W analysis:

- **PDF fits**: Fixed-order QCD at NNLO "standard", usually supplemented with higher order EWK corrections, fully differential FEWZ, DYNNLO (and others), actual fits often done with NLO-to-NNLO K-factors or other approximation

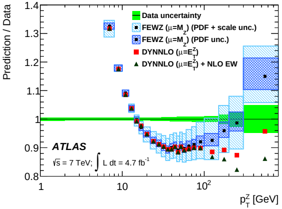

- **m_W@Tevatron & CT-group PDF fits**: resummed predictions at NNLO+(N)NLO with ResBos
- **m_W@ATLAS**: hybrid prediction with fixed-order QCD at NNLO in full phase space (rapidity + angular correlations) + Parton shower MC for detector level

Does the mismatch between two approaches matter?

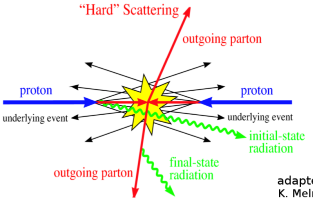

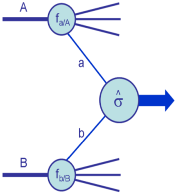

adapted from
K. Melnikov, QCD@LHC 2016

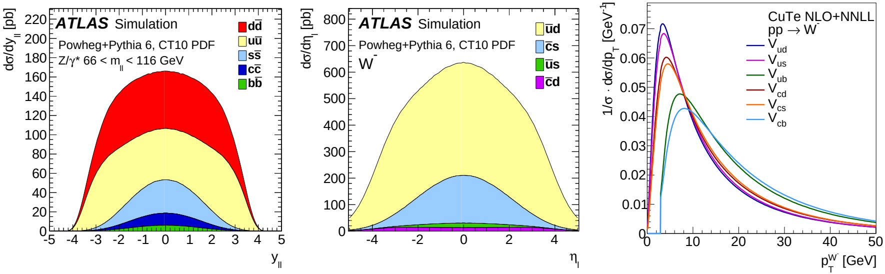

W, Z production at LO determined by sum of different $q\bar{q}$ combinations weighted by different electro-weak couplings (and CKM elements for $W^{\pm}$)

- Different composition of flavours than constrained by the HERA dataset
- W-boson mass measurement subject to significant PDF uncertainties due to large cs component $\rightarrow$ propagates also to W-boson p_T spectrum, which is harder for heavy-flavour induced component

Validation and/or constraints from precise $W, Z/\gamma^*$ measurements crucial to constrain light-flavour decomposition

W and Z/γ^* Measurements

Wide range of precise measurements at LHC (mostly $\sqrt{s} = 7, 8$ TeV) and Tevatron available, will highlight some recent examples of the last 1–2 years

- ATLAS differential $W, Z/\gamma^*$ 7 TeV: $e + \mu$, QCD analysis [arXiv:1612.03016]
- ATLAS $Z, t\bar{t}$ 7, 8, 13 TeV: $e + \mu$, PDF study [arXiv:1612.03636, accepted by JHEP]
- ATLAS differential $Z/\gamma^*, m_{\ell\ell} > 116$ GeV, 8 TeV: $e + \mu$, χ^2 vs. PDF sets and γ PDF [JHEP 08 (2016) 009, arXiv:1701.08553]
- CMS differential $Z/\gamma^*, 20 < m_{\ell\ell} < 1500$ GeV, 8 TeV: $e + \mu$ [EPJC (2015) 75:147]
- CMS differential $W^{\pm}$: 8 TeV: μ, PDF fit [EPJC (2016) 76:469]
- LHCb W, Z: μ, e [JHEP 01 (2016) 155, JHEP 10 (2016) 030]
- CDF + D0 dif. $W^{\pm}$ asymmetry and Z: xFitter study [EPJC (2015) 75:458]

More effort to ensure these different data sets contribute to a consistent PDF determination, e.g. more direct comparison of experimental data?

ATLAS 7 TeV: σ_{fid} and ratios vs. Theory

[arXiv:1612.03016]

- Predictions obtained with DYNNLO with fiducial lepton cuts matching the detector; NLO EWK beyond QED FSR calculated with SANC & FEWZ
- Ratios of integrated fiducial cross sections more precise than most PDF sets: $W^{\pm}$ well described, W/Z ratio systematically different ($\rightarrow$ strange PDF)

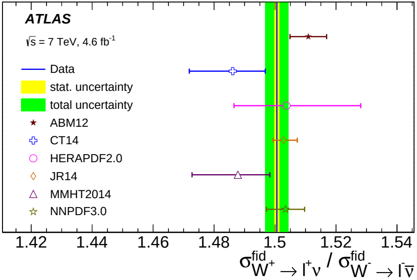

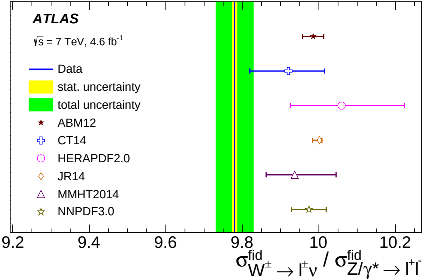

- Absolute cross-sections reveal that CT/NNPDF/MMHT PDFs tend to be systematically low, although within the luminosity uncertainty of 1.8%

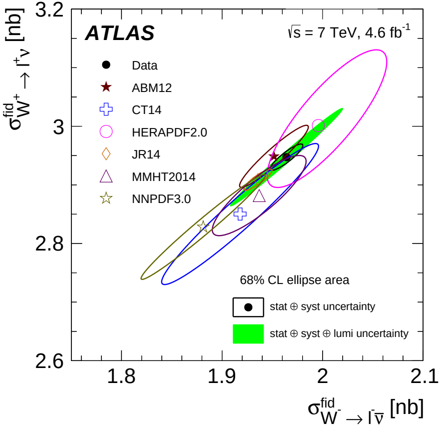

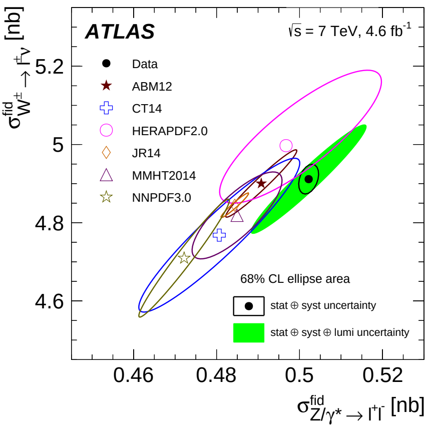

ATLAS $7-13$ TeV: $Z/t\bar{t}$

[arXiv:1612.03636]

- Study of integrated Z and $t\bar{t}$ tests $q\bar{q}$ vs. gg luminosties
- CT/NNPDF/MMHT PDFs are systematically shifted, while HERAPDF and ATLAS-epWZ12 do better; ABM12 different for $t\bar{t}$

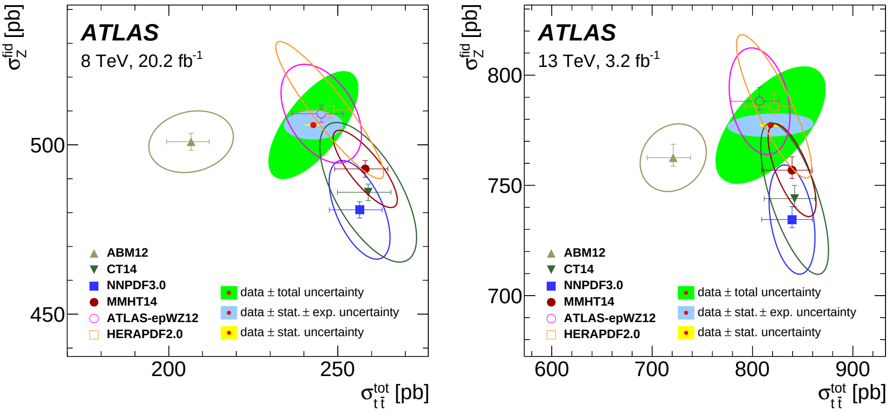

ATLAS 7 − 13 TeV: $Z/t\bar{t}$

[arXiv:1612.03636]

- Study of integrated Z and $t\bar{t}$ tests $q\bar{q}$ vs. gg luminosties
- CT/NNPDF/MMHT PDFs are systematically shifted, while HERAPDF and ATLAS-epWZ12 do better; ABM12 different for $t\bar{t}$

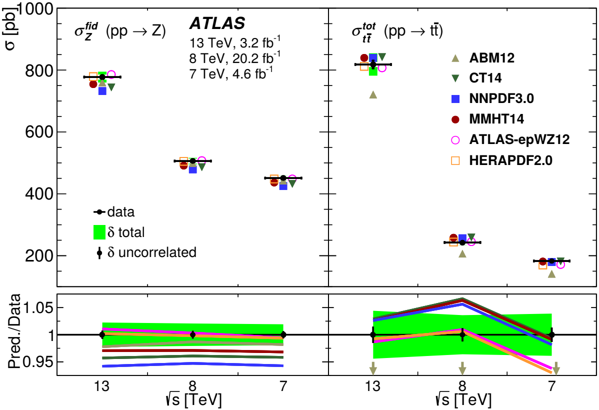

	ATLAS-epWZ12	CT14	MMHT14	NNPDF3.0	HERAPDF2.0	ABM12
χ^2/NDF	8.3 / 6	15 / 6	13 / 6	17 / 6	10 / 6	25 / 6
p-value	0.22	0.02	0.05	0.01	0.11	$<$ 0.001

Impact of $pp/p\bar{p} \to$ jet data [S. Glazov @ PrecisionVietnam2016]

- Adding e.g. ATLAS jet data to HERAPDF2.0-like PDF fit reduces low x quark-sea (Σ) and increase medium/high x gluon:
  $\to$ decrease σ_Z, increase $\sigma_{t\bar{t}}$ — disfavoured by LHC $W, Z, t\bar{t}$ data, possibly resolved by using NNLO for jets?
- General trend for most data on jet production in $pp/p\bar{p}$, except CMS jet data

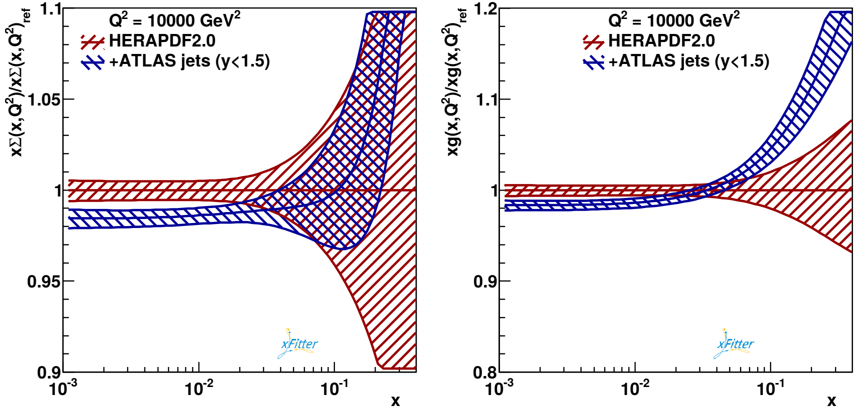

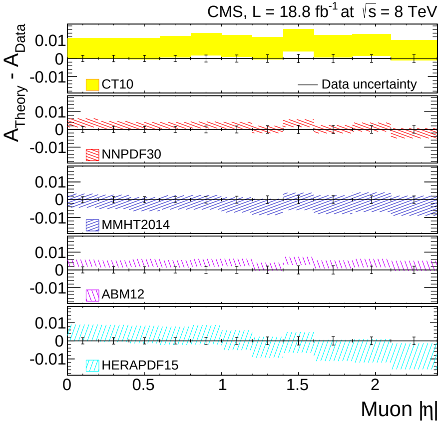

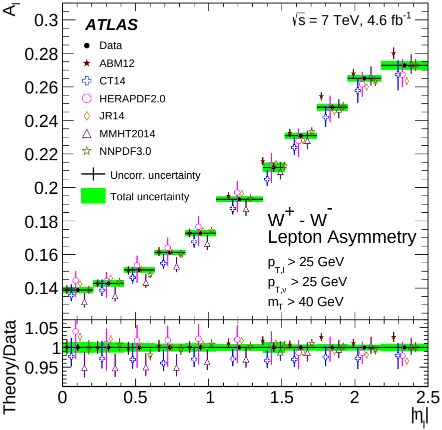

- All modern PDF sets reproduce the data up to $\sim 1 - 2\sigma$ trends in central values
- Data generally more precise than theory *to* further PDF constraining-power

CMS/ATLAS 8, 7 TeV: diff. Z

[EPJC (2015) 75:147, arXiv:1612.03016]

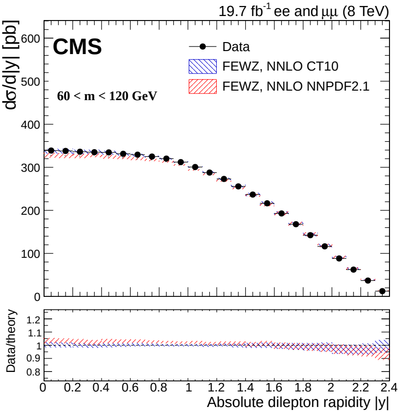

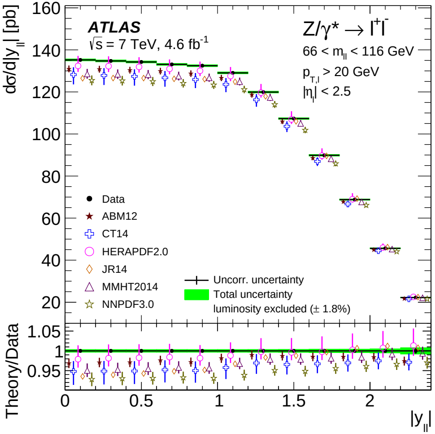

- Data uncertainty typically less than PDF unc., many PDF sets struggle to describe the (ATLAS) data

ATLAS 7 TeV: data/theory χ^2

[arXiv:1612.03016]

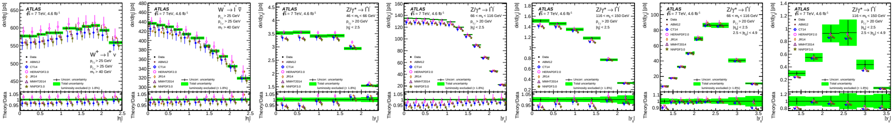

- Quantitative χ^2 analysis of theory/data agreement using several $W^\pm, Z/\gamma^*$ differential distributions and full correlation information
- Challenge for theory & PDFs: CT14 ($\chi^2/\mathrm{n.d.f.} = 103/61$) best, NNPDF3.0 ($\chi^2/\mathrm{n.d.f.} = 147/61$) worst
- Older CT10 gives $\chi^2/\mathrm{n.d.f.} = 101/61$ – used as baseline for ATLAS m_W

Data set	n.d.f.	ABM12	CT14	MMHT14	NNPDF3.0	ATLAS-epWZ12
$W^+ \to \ell^+\nu$	11	11|21	10|26	11|37	11|18	12|15
$W^- \to \ell^-\bar{\nu}$	11	12|20	8.9|27	8.1|31	12|19	7.8|17
$Z/\gamma^* \to \ell\ell$ ($m_{\ell\ell} = 46 - 66$ GeV)	6	17|21	11|30	18|24	21|22	28|36
$Z/\gamma^* \to \ell\ell$ ($m_{\ell\ell} = 66 - 116$ GeV)	12	24|51	16|66	20|116	14|109	18|26
Forward $Z/\gamma^* \to \ell\ell$ ($m_{\ell\ell} = 66 - 116$ GeV)	9	7.3|9.3	10|12	12|13	14|18	6.8|7.5
$Z/\gamma^* \to \ell\ell$ ($m_{\ell\ell} = 116 - 150$ GeV)	6	6.1|6.6	6.3|6.1	5.9|6.6	6.1|8.8	6.7|6.6
Forward $Z/\gamma^* \to \ell\ell$ ($m_{\ell\ell} = 116 - 150$ GeV)	6	4.2|3.9	5.1|4.3	5.6|4.6	5.1|5.0	3.6|3.5
Correlated χ^2		57|90	39|123	43|167	69|157	31|48
Total χ^2	61	136|222	103|290	118|396	147|351	113|159

χ^2 {with | without} uncertainties from PDF sets

ATLAS 7 TeV: QCD fit analysis

[arXiv:1612.03016]

- Use the final HERA II DIS data set and new ATLAS W and Z data to derive a new PDF set: ATLAS-epWZ16
- NNLO QCD can describe data: nominal $\chi^2 = 108/61$
- W, Z predictions at half of the conventional scales $\mu_r = \mu_f = 0.5 m_{\ell\ell}$ improves fit χ^2 significantly: $\chi^2 = 85/61$
- Perturbative series for $gg \to H$ know to N^{3}LO – converges better for $m_H/2$; also $t\bar{t}$ typically calculated at scales well below $2m_t$

μ_r	μ_f	χ^2/n.d.f. Total	χ^2/n.d.f. ATLAS
1	1	1321 / 1102	108 / 61
1/2	1/2	1297 / 1102	85 / 61
2	2	1329 / 1102	115 / 61
1	1/2	1307 / 1102	94 / 61
1	2	1312 / 1102	100 / 61
1/2	1	1304 / 1102	94 / 61
2	1	1321 / 1102	107 / 61

$gg \to H$ @ N^{3}LO [PRL 114 (2015) 212001]

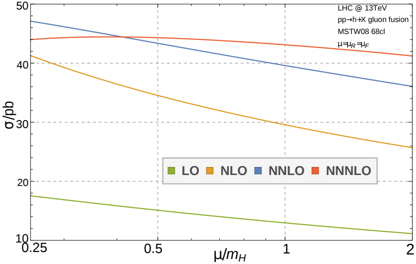

Fixed-order theory limitations [Uta Klein, Misha Lisovyi]

- QCD predictions in fiducial phase space: lepton acceptance cuts on p_T^ℓ and η^ℓ introduce additional "features"/uncertainties
- E.g. W^+ cross section in ATLAS fiducial phase space $|\eta^\ell| < 2.5$, $p_T^\nu > 25$ GeV, $p_T^{\ell+} > 25$ GeV, $m_T > 40$ GeV
- Scan $p_T^{\ell+} > 20..30$ GeV naive expectation of continuous behaviour across "symmetric configuration" $p_T^\nu = p_T^{\ell+}$ violated significantly at NLO; at NNLO behaviour smoother, but FEWZ makes an unphysical "jump"

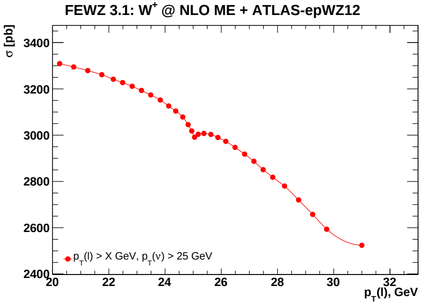

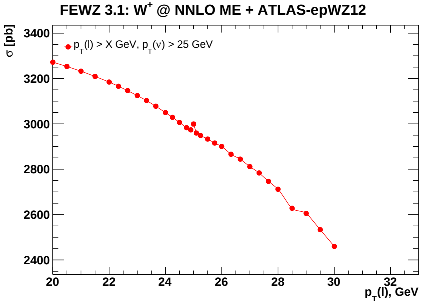

Fixed-order theory limitations

[Uta Klein, Misha Lisovyi]

- Size of jump dependent on kinematic region
  - $\sim 2\%$ for lower mass γ^* ($2p^{\ell}_{T,cut} \sim m_{\ell\ell}$, "LM CC")
  - $< 0.2\%$ for Z-peak and above ($2p^{\ell}_{T,cut} \ll m_{\ell\ell}$, "Z CC", "Z HM")
  - $\sim 0.5\%$ for kinematically more resctricted central-forward selection ("Z CF", "HM CF")
  - $0.7 - 1.0\%$ for $W^{\pm}$
- Size of jump for many regions at similar level as measurement uncertainty
- DYNNLO on the other hand is effectively "smooth"

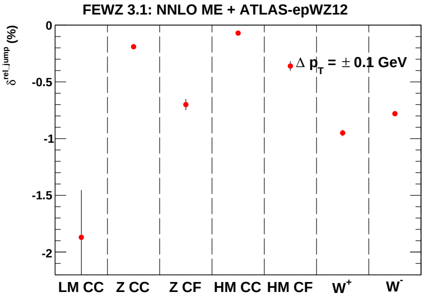

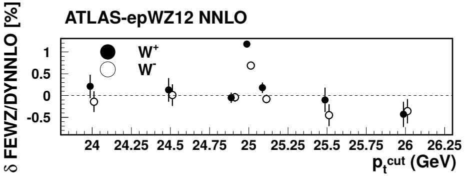

The strange-quark density

[arXiv:1612.03016]

- Confirmation of result with ATLAS 2010 W, Z data of large strange-quark sea at low $Q^2 = 1.9$ GeV^2 and low $x = 0.023$ with significantly reduced experimental uncertainty:
  $r_s = \bar{s}/\bar{d} = 1.19 \pm 0.07\,(\mathrm{exp}) \pm 0.16\,(\mathrm{fit + thy})$
- Uncertainties from QCD scale and FEWZ/DYNNLO now larger than experimental uncertainties
- Most PDF sets feature significantly suppressed strange-quark density

	$r_s = \frac{s+\bar{s}}{2\bar{d}}$	$R_s = \frac{s+\bar{s}}{\bar{u}+\bar{d}}$
Central value	1.19	1.13
Experimental data	± 0.07	± 0.05
Model (m_b, $Q^2_{\rm min}$, Q^2_0 & m_c)	± 0.02	± 0.02
Parameterization	$^{+0.02}_{-0.10}$	$^{+0.01}_{-0.06}$
α_S	$^{+0.00}_{-0.01}$	± 0.01
Beam energy E_p	± 0.03	$^{+0.01}_{-0.02}$
EW corrections	± 0.01	± 0.00
QCD scales	$^{+0.08}_{-0.10}$	$^{+0.06}_{-0.07}$
FEWZ 3.1b2	$+0.10$	$+0.08$
Total uncertainty	$^{+0.15}_{-0.16}$	± 0.11

ATLAS 2011 W, Z data + HERA II

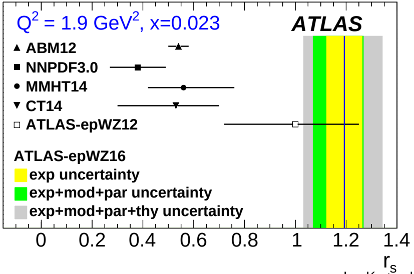

ATLAS 2010 W, Z data + HERA I

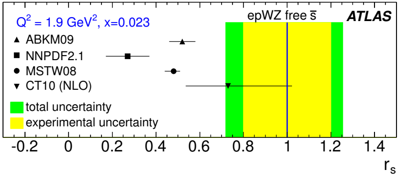

The strange-quark density

[arXiv:1612.03016, EPJC (2016) 76:471]

- Tension with most PDF sets due to neutrino–fixed target DIS di-muon data, which favours $r_s \sim 0.5$ at $Q^2 = 1.9\,\text{GeV}^2$?
- LHC W+charm data (7 TeV) not yet precise enough and currently NLO only: ATLAS $r_s^{\text{W+c}} = 0.96 \pm 0.28$, CMS $r_s^{\text{W+c}} \sim 0.7 \pm 0.2$ ($\rightarrow$ need more data and NNLO)

adapted from EPJC (2016) 76:471 + arXiv:1612.03016

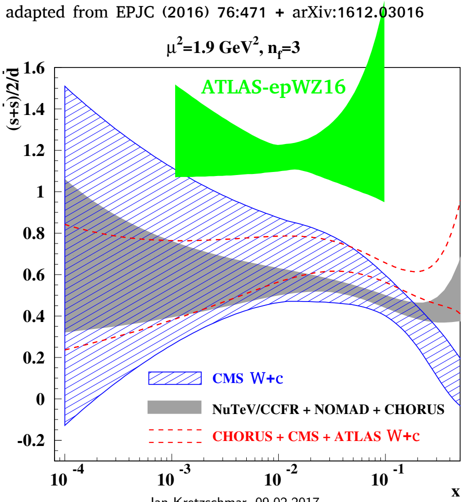

The strange-quark density

[arXiv:1612.03016, EPJC (2016) 76:471]

- Tension with most PDF sets due to neutrino–fixed target DIS di-muon data, which favours $r_s \sim 0.5$ at $Q^2 = 1.9\,\text{GeV}^2$?
- LHC W+charm data (7 TeV) not yet precise enough and currently NLO only: ATLAS $r_s^{\mathrm{W+c}} = 0.96 \pm 0.28$, CMS $r_s^{\mathrm{W+c}} \sim 0.7 \pm 0.2$ ($\rightarrow$ need more data and NNLO)

adapted from EPJC (2016) 76:471 + arXiv:1612.03016

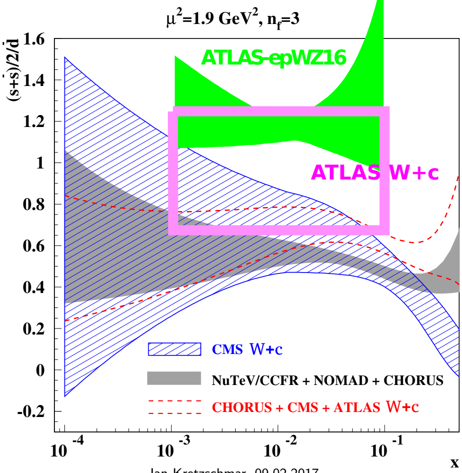

Valence quarks

- Valence quark uncertainties affect amount of W-polarisation, an important source of uncertainty on m_W at LHC
- More constraints from diff. W^+–W^- cross sections/asymmetries and Z/γ^*
- e.g. MMHT2014 already contains several relevant Tevatron and LHC sets, some more information available:

LHCb $Z, W^{\pm}$ as included in ABMP16 fit [arXiv:1701.05838]

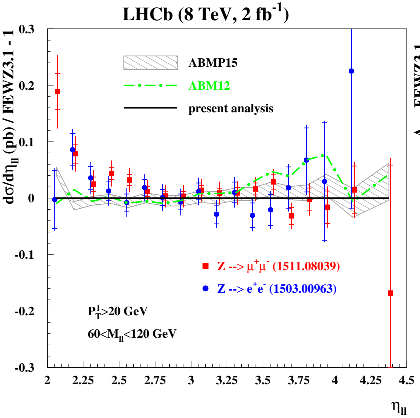

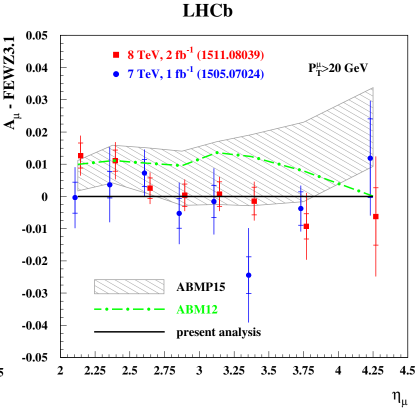

Valence quarks

- Valence quark uncertainties affect amount of W-polarisation, an important source of uncertainty on m_W at LHC
- More constraints from diff. W^+–W^- cross sections/asymmetries and Z/γ^*
- e.g. MMHT2014 already contains several relevant Tevatron and LHC sets, some more information available:

CMS fit to HERA + $W^\pm$ [EPJC (2016) 76:469]

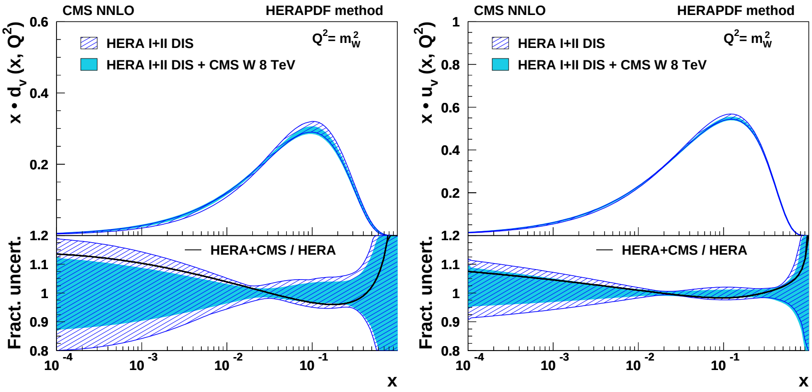

Valence quarks

- Valence quark uncertainties affect amount of W-polarisation, an important source of uncertainty on m_W at LHC
- More constraints from diff. W^+–W^- cross sections/asymmetries and Z/γ^*
- e.g. MMHT2014 already contains several relevant Tevatron and LHC sets, some more information available:

profiling MMHT2014 with additional

Tevatron data [EPJC (2015) 75:458] ATLAS data [arXiv:1612.03016]

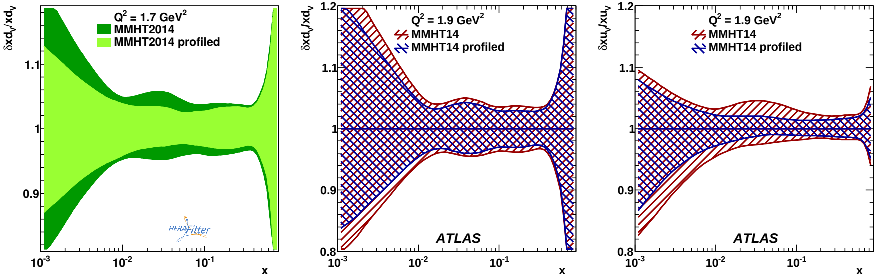

Summary

- PDF are important for m_W
- Precise data W,Z production data available to validate & constrain PDFs for m_W – requires some effort to compare data directly and incorporate in PDF fits
- Some issues in the use of W,Z data:
  - Mismatch between tools used in PDF fits and m_W analysis
  - Theory uncertainties now at same level as experimental errors
  - $\rightarrow$ N^{3}LO for DIS and DY?
- CT/NNPDF/MMHT PDFs reproduce $Z/t\bar{t}$ ratio worse than PDFs pased on DIS and DY data, probably due to jet data $\rightarrow$ improvement with NNLO for jets?
- Recent ATLAS analysis of W, Z data results in large, unsuppressed strange-quark density – contradiction with neutrino data?

Backup - A largely random collection

DGLAP

- PDF Q^2 evolution: *DGLAP equations* [Altarelli and Parisi, 1977]

$$\frac{dq^i(x,t)}{dt} = \frac{\alpha(t)}{2\pi}\int_x^1 \frac{dy}{y}\left[\sum_j^{2f} q^j(y,t)\, P_{q^i q^j}\left(\frac{x}{y}\right) + G(y,t)\, P_{q^i G}\left(\frac{x}{y}\right)\right] \qquad (22)$$

$$\frac{dG(x,t)}{dt} = \frac{\alpha(t)}{2\pi}\int_x^1 \frac{dy}{y}\left[\sum_j^{2f} q^j(y,t)\, P_{G q^j}\left(\frac{x}{y}\right) + G(y,t)\, P_{GG}\left(\frac{x}{y}\right)\right] \qquad (23)$$

$(t = \ln Q^2/Q_0^2)$

- Full LHC W, Z production x range only covered by HERA NC data

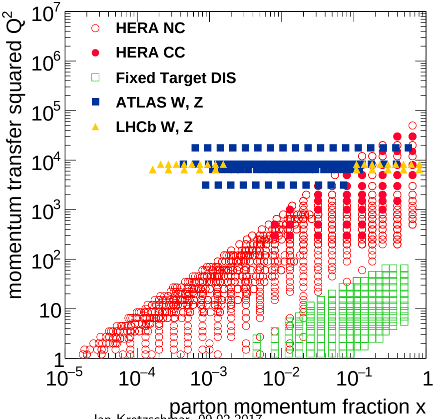

Cross-section measurements

- $W^+ \to \ell^+\nu$ and $W^- \to \ell^-\nu$ measured integrated and as function of charged lepton rapidity $|\eta_\ell|$: typical precision $0.6 - 1.0\%$
- $Z/\gamma^* \to \ell\ell$ measured integrated and as function of di-lepton rapidity $|y_{\ell\ell}|$ and di-lepton mass $m_{\ell\ell}$: typical precision 0.4%, forward Z 2.3%

Electron channels

	$\delta\sigma_{W+}$ [%]	$\delta\sigma_{W-}$ [%]	$\delta\sigma_{Z}$ [%]	$\delta\sigma_{\text{forward } Z}$ [%]
Trigger efficiency	0.03	0.03	0.05	0.05
Reconstruction efficiency	0.12	0.12	0.20	0.13
Identification efficiency	0.09	0.09	0.16	0.12
Forward identification efficiency	–	–	–	1.51
Isolation efficiency	0.03	0.03	–	0.04
Charge misidentification	0.04	0.06	–	–
Electron p_T resolution	0.02	0.03	0.01	0.01
Electron p_T scale	0.22	0.18	0.08	0.12
Forward electron p_T scale + resolution	–	–	–	0.18
E_T^{miss} soft term scale	0.14	0.13	–	–
E_T^{miss} soft term resolution	0.06	0.04	–	–
Jet energy scale	0.04	0.02	–	–
Jet energy resolution	0.11	0.15	–	–
Signal modelling (matrix-element generator)	0.57	0.64	0.03	1.12
Signal modelling (parton shower and hadronization)	0.24	0.25	0.18	1.25
PDF	0.10	0.12	0.09	0.06
Boson p_T	0.22	0.19	0.01	0.04
Multijet background	0.55	0.72	0.03	0.05
Electroweak+top background	0.17	0.19	0.02	0.14
Background statistical uncertainty	0.02	0.03	<0.01	0.04
Unfolding statistical uncertainty	0.03	0.04	0.04	0.13
Data statistical uncertainty	0.04	0.05	0.10	0.18
Total experimental uncertainty	0.94	1.08	0.35	2.29
Luminosity			1.8	

Muon channels

	$\delta\sigma_{W+}$ [%]	$\delta\sigma_{W-}$ [%]	$\delta\sigma_{Z}$ [%]
Trigger efficiency	0.08	0.07	0.05
Reconstruction efficiency	0.19	0.17	0.30
Isolation efficiency	0.10	0.09	0.15
Muon p_T resolution	0.01	0.01	<0.01
Muon p_T scale	0.18	0.17	0.03
E_T^{miss} soft term scale	0.19	0.19	–
E_T^{miss} soft term resolution	0.10	0.09	–
Jet energy scale	0.09	0.12	–
Jet energy resolution	0.11	0.16	–
Signal modelling (matrix-element generator)	0.12	0.06	0.04
Signal modelling (parton shower and hadronization)	0.14	0.17	0.22
PDF	0.09	0.12	0.07
Boson p_T	0.18	0.14	0.04
Multijet background	0.33	0.27	0.07
Electroweak+top background	0.19	0.24	0.02
Background statistical uncertainty	0.03	0.04	0.01
Unfolding statistical uncertainty	0.03	0.03	0.02
Data statistical uncertainty	0.04	0.04	0.08
Total experimental uncertainty	0.61	0.59	0.43
Luminosity		1.8	

ATLAS *W*

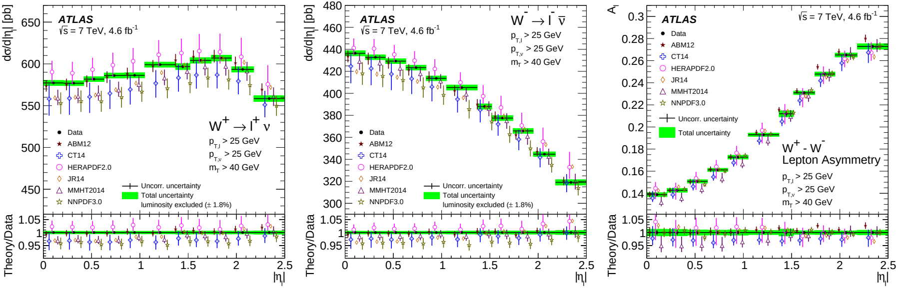

ATLAS
√s = 7 TeV, 4.6 fb-1
W+ → l+ ν
pT,l > 25 GeV
pT,ν > 25 GeV
mT > 40 GeV
Data
ABM12
CT14
HERAPDF2.0
JR14
MMHT2014
NNPDF3.0
Uncorr. uncertainty
Total uncertainty
luminosity excluded (± 1.8%)
dσ/d|ηl| [pb]
Theory/Data
|ηl|
W- → l- ν̄
W+ - W-
Lepton Asymmetry
Al

ATLAS *Z*

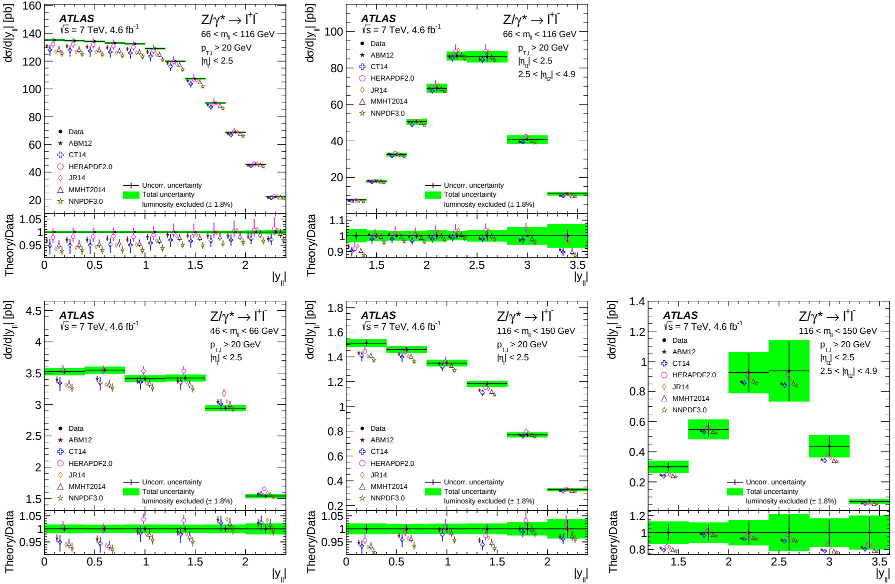
ATLAS
√s = 7 TeV, 4.6 fb-1
Z/γ* → l+l-
66 < mll < 116 GeV
pT,l > 20 GeV
|ηl| < 2.5
2.5 < |ηl2| < 4.9
46 < mll < 66 GeV
116 < mll < 150 GeV
Data
ABM12
CT14
HERAPDF2.0
JR14
MMHT2014
NNPDF3.0
Uncorr. uncertainty
Total uncertainty
luminosity excluded (± 1.8%)
dσ/d|yll| [pb]
Theory/Data
|yll|

PDF profiling

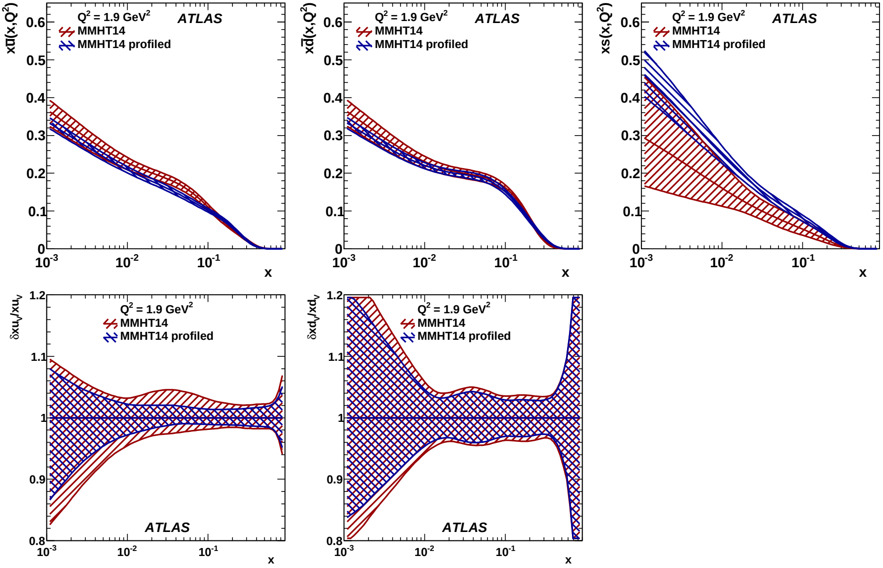

ATLAS-epWZ16

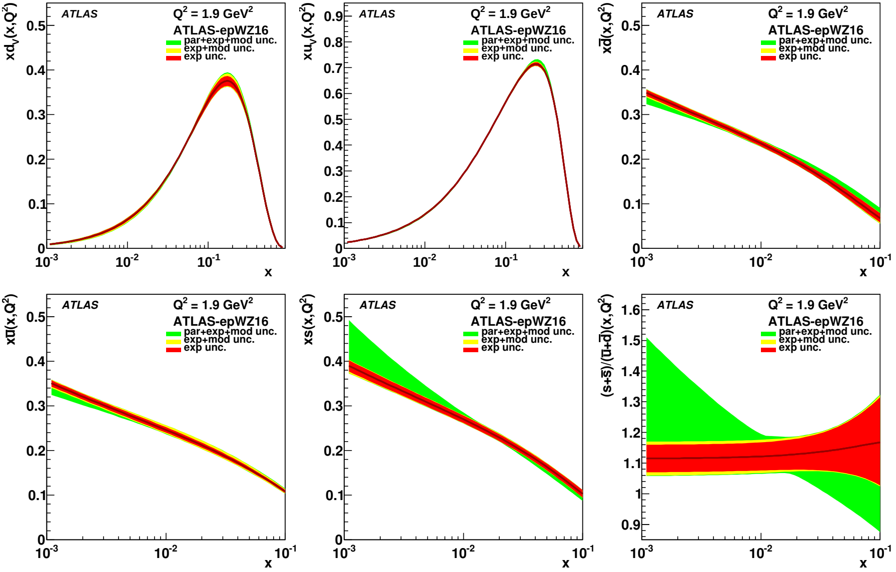

Strange

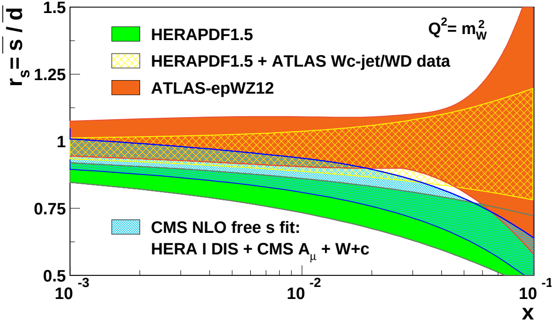
$r_s = \bar{s}/\bar{d}$
$Q^2 = m_W^2$
HERAPDF1.5
HERAPDF1.5 + ATLAS Wc-jet/WD data
ATLAS-epWZ12
CMS NLO free s fit:
HERA I DIS + CMS A_μ + W+c
1.5
1.25
1
0.75
0.5
10^{-3}
10^{-2}
10^{-1}
x

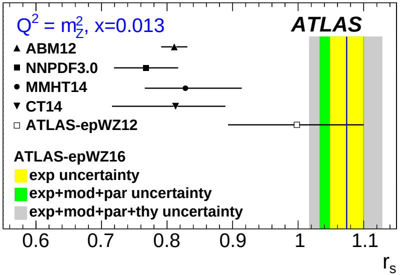
$Q^2 = m_Z^2$, x=0.013
ATLAS
ABM12
NNPDF3.0
MMHT14
CT14
ATLAS-epWZ12
ATLAS-epWZ16
exp uncertainty
exp+mod+par uncertainty
exp+mod+par+thy uncertainty
0.6
0.7
0.8
0.9
1
1.1
r_s

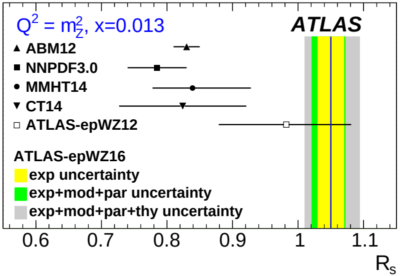
$Q^2 = m_Z^2$, x=0.013
ATLAS
ABM12
NNPDF3.0
MMHT14
CT14
ATLAS-epWZ12
ATLAS-epWZ16
exp uncertainty
exp+mod+par uncertainty
exp+mod+par+thy uncertainty
0.6
0.7
0.8
0.9
1
1.1
R_s

Strange

PDF parameterised at starting scale Q_0^2 with 15 free parameters

$$
\begin{aligned}
xu_v(x) &= A_{u_v} x^{B_{u_v}} (1-x)^{C_{u_v}} (1 + E_{u_v} x^2)\,, \\
xd_v(x) &= A_{d_v} x^{B_{d_v}} (1-x)^{C_{d_v}}\,, \\
x\bar{u}(x) &= A_{\bar{u}} x^{B_{\bar{u}}} (1-x)^{C_{\bar{u}}}\,, \\
x\bar{d}(x) &= A_{\bar{d}} x^{B_{\bar{d}}} (1-x)^{C_{\bar{d}}}\,, \\
xg(x) &= A_g x^{B_g} (1-x)^{C_g} - A'_g x^{B'_g} (1-x)^{C'_g}\,, \\
x\bar{s}(x) &= A_{\bar{s}} x^{B_{\bar{s}}} (1-x)^{C_{\bar{s}}}\,,
\end{aligned}
$$

W, Z Combination

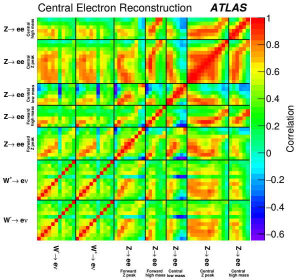

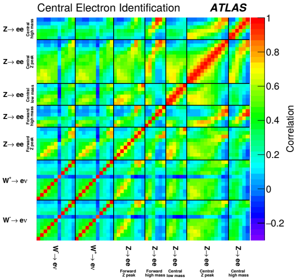

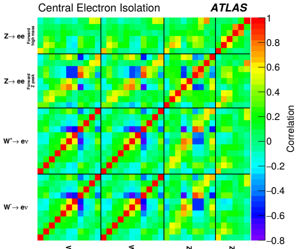

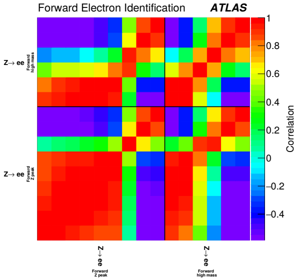

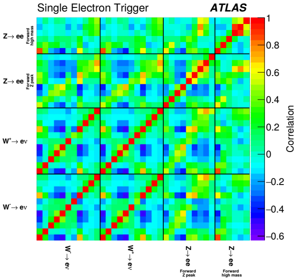

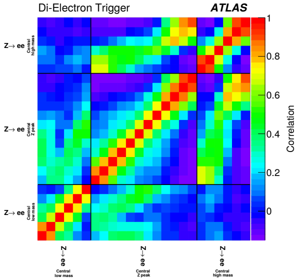

W, Z Combination

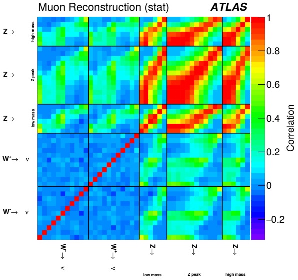

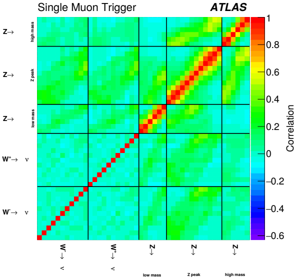

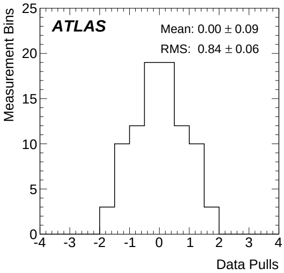

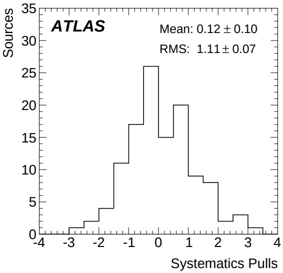

W, Z Combination

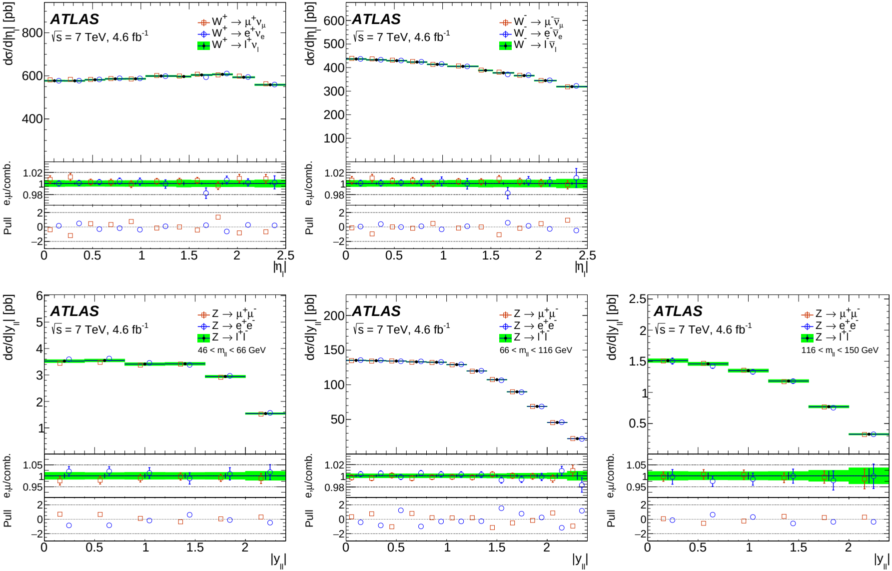

The five-dimensional DY cross sections

- Description of production and decay of single $W^{\pm} \to \ell\nu$ and $Z/\gamma^* \to \ell\ell$ depends on five kinematic variables:
  - Boson 4-vector: di-lepton mass $m_{\ell\ell}$, transverse momentum $p_{T,\ell\ell}$ and rapidity $y_{\ell\ell}$
  - Spin-1 of $W/Z/\gamma^*$ bosons and EWK coupling effects the two decay leptons have non-trivial angular correlations (θ_{CS} and ϕ_{CS})
- Can be factorised as

$$\frac{\mathrm{d}\sigma}{\mathrm{d}m_{\ell\ell}\mathrm{d}p_{T,\ell\ell}\mathrm{d}y_{\ell\ell}}\left[1+\cos^2\theta_{CS}+\sum_{i=0}^{7}A_i(m,p_T,y)f_i(\theta_{CS},\phi_{CS})\right]$$

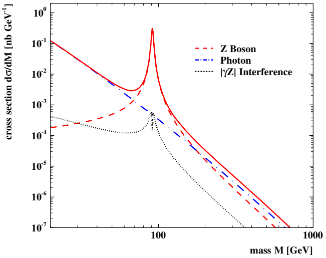

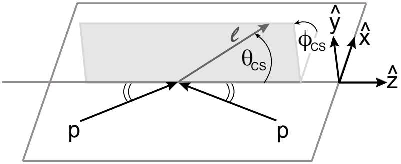

$A_{\rm FB}$ — — $\sin^2\theta_W$ **constraint**

arXiv:1507.02470

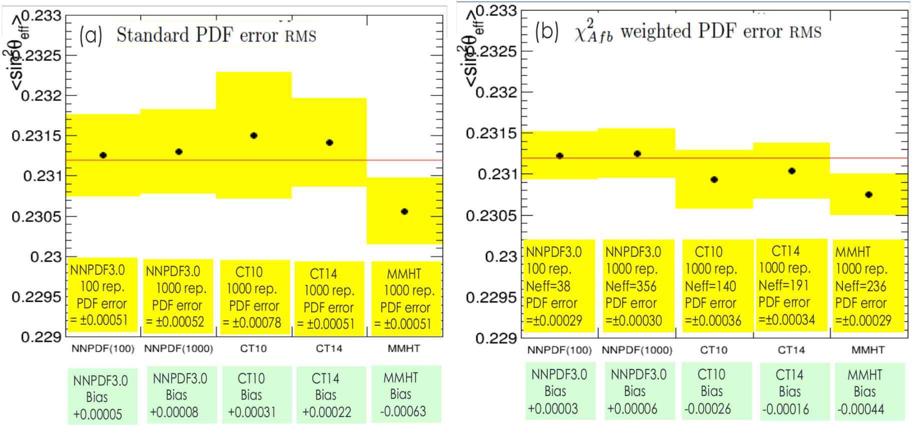

CDF

Source	Uncertainty
Lepton energy scale and resolution	7
Recoil energy scale and resolution	6
Lepton tower removal	2
Backgrounds	3
PDFs	10
$p_T(W)$ model	5
Photon radiation	4
Statistical	12
Total	19

ATLAS

Stat. Unc.	Muon Unc.	Elec. Unc.	Recoil Unc.	Bckg. Unc.	QCD Unc.	EWK Unc.	PDF Unc.	Total Unc.	
6.8	6.6	6.4	2.9	4.5	8.3	5.5	9.2	18.5	[MeV]

ATLAS mass difference

Channel	$m_{W^+} - m_{W^-}$ [MeV]	Stat. Unc.	Muon Unc.	Elec. Unc.	Recoil Unc.	Bckg. Unc.	QCD Unc.	EW Unc.	PDF Unc.	Total Unc.
$W \to e\nu$	−29.7	17.5	0.0	4.9	0.9	5.4	0.5	0.0	24.1	30.7
$W \to \mu\nu$	−28.6	16.3	11.7	0.0	1.1	5.0	0.4	0.0	26.0	33.2
Combined	−29.2	12.8	3.3	4.1	1.0	4.5	0.4	0.0	23.9	28.0

PDFs and Deep Inelastic Scattering

[EPJC (2015) 75:580, EPJC (2009) 63:189]

- DIS experiments at SLAC in 1969 ($ep \to eX$) found cross section to be $\sim$independent of momentum transfer Q^2: proton consists of point-like *quarks*
- Further precise measurements, e.g. at HERA *ep* collider, over wide range of x, Q^2: neutral current (γ^* exchange) constrains $\sum e_q^2(q+\bar{q})$, at low momentum fraction x strong *scaling violations* due to gluons
- A big unknown is the flavour decomposition of light-quark sea at $x < 10^{-2}$: $\bar{u} \sim \bar{d}$, strange suppressed?

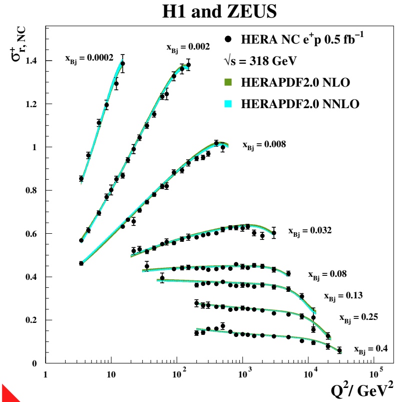

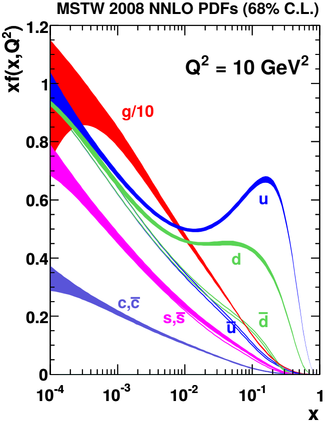

Integrated cross-section results and combination

- Integrated cross sections measured to 0.6 – 1.0% for W and 0.4% for Z
- Overall correlated 1.8% luminosity uncertainty
- Combination interpreted as test of $e - \mu$ universality: most precise test for on-shell W

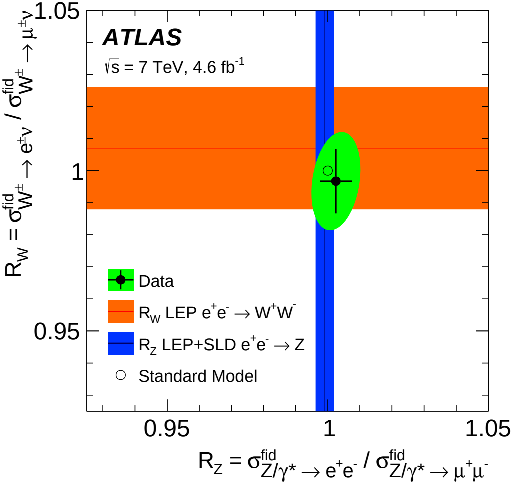

Fully differential physics model for DY

- Factorisation of five-dimensional DY cross section allows reweighting

$$\frac{\mathrm{d}\sigma}{\mathrm{d}m_{\ell\ell}\mathrm{d}p_{T,\ell\ell}\mathrm{d}y_{\ell\ell}}\left[1+\cos^2\theta_{CS}+\sum_{i=0}^{7}A_i(m_{\ell\ell},p_{T,\ell\ell},y_{\ell\ell})f_i(\theta_{CS},\phi_{CS})\right]$$

- Higher order QED effects simulated, missing EWK pieces as systematics
- $m_{\ell\ell}$: BW-resonance (+ γ^* effects for $\ell^+\ell^-$)
- $y_{\ell\ell}$, angular coefficients A_i: fixed-order NNLO QCD with CT10, validated by measured W, Z cross-sections and $Z \to \ell\ell$ angular correlations (JHEP08(2016)159)
- $p_{T,\ell\ell}$: needs resummation or parton shower

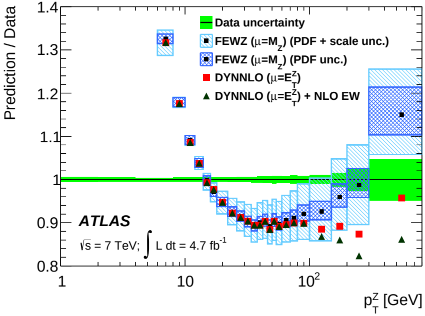

W-boson mass result per category

- Analysis binned in $|\eta|$ and $W^{\pm}$-charge categories and fit performed in both p_T^ℓ and m_T
- $P(\chi^2)$ distribution over all fit categories: uncertainties well calibrated
- Combination including correlations: $\chi^2/\text{n.d.f.} = 29/27$

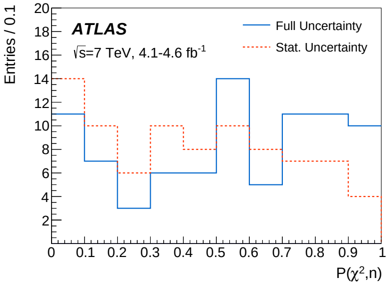

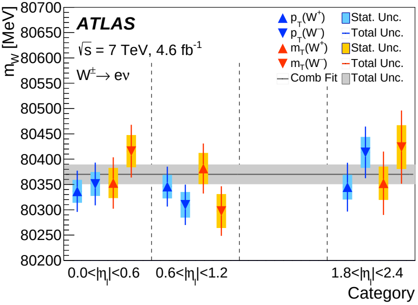

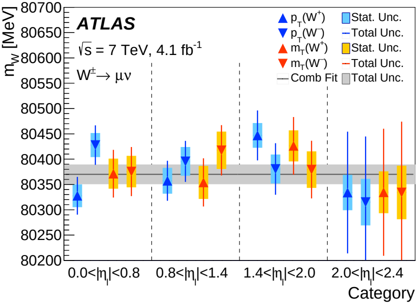

W-boson mass result per category

Channel m_T-Fit	m_W [MeV]	Stat. Unc.	Muon Unc.	Elec. Unc.	Recoil Unc.	Bckg. Unc.	QCD Unc.	EWK Unc.	PDF Unc.	Total Unc.
$W^+ \to \mu\nu, \lvert\eta\rvert < 0.8$	80371.3	29.2	12.4	0.0	15.2	8.1	9.9	3.4	28.4	47.1
$W^+ \to \mu\nu, 0.8 < \lvert\eta\rvert < 1.4$	80354.1	32.1	19.3	0.0	13.0	6.8	9.6	3.4	23.3	47.6
$W^+ \to \mu\nu, 1.4 < \lvert\eta\rvert < 2.0$	80426.3	30.2	35.1	0.0	14.3	7.2	9.3	3.4	27.2	56.9
$W^+ \to \mu\nu, 2.0 < \lvert\eta\rvert < 2.4$	80334.6	40.9	112.4	0.0	14.4	9.0	8.4	3.4	32.8	125.5
$W^- \to \mu\nu, \lvert\eta\rvert < 0.8$	80375.5	30.6	11.6	0.0	13.1	8.5	9.5	3.4	30.6	48.5
$W^- \to \mu\nu, 0.8 < \lvert\eta\rvert < 1.4$	80417.5	36.4	18.5	0.0	12.2	7.7	9.7	3.4	22.2	49.7
$W^- \to \mu\nu, 1.4 < \lvert\eta\rvert < 2.0$	80379.4	35.6	33.9	0.0	10.5	8.1	9.7	3.4	23.1	56.9
$W^- \to \mu\nu, 2.0 < \lvert\eta\rvert < 2.4$	80334.2	52.4	123.7	0.0	11.6	10.2	9.9	3.4	34.1	139.9
$W^+ \to e\nu, \lvert\eta\rvert < 0.6$	80352.9	29.4	0.0	19.5	13.1	15.3	9.9	3.4	28.5	50.8
$W^+ \to e\nu, 0.6 < \lvert\eta\rvert < 1.2$	80381.5	30.4	0.0	21.4	15.1	13.2	9.6	3.4	23.5	49.4
$W^+ \to e\nu, 1{,}8 < \lvert\eta\rvert < 2.4$	80352.4	32.4	0.0	26.6	16.4	32.8	8.4	3.4	27.3	62.6
$W^- \to e\nu, \lvert\eta\rvert < 0.6$	80415.8	31.3	0.0	16.4	11.8	15.5	9.5	3.4	31.3	52.1
$W^- \to e\nu, 0.6 < \lvert\eta\rvert < 1.2$	80297.5	33.0	0.0	18.7	11.2	12.8	9.7	3.4	23.9	49.0
$W^- \to e\nu, 1.8 < \lvert\eta\rvert < 2.4$	80423.8	42.8	0.0	33.2	12.8	35.1	9.9	3.4	28.1	72.3
p_T-Fit										
$W^+ \to \mu\nu, \lvert\eta\rvert < 0.8$	80327.7	22.1	12.2	0.0	2.6	5.1	9.0	6.0	24.7	37.3
$W^+ \to \mu\nu, 0.8 < \lvert\eta\rvert < 1.4$	80357.3	25.1	19.1	0.0	2.5	4.7	8.9	6.0	20.6	39.5
$W^+ \to \mu\nu, 1.4 < \lvert\eta\rvert < 2.0$	80446.9	23.9	33.1	0.0	2.5	4.9	8.2	6.0	25.2	49.3
$W^+ \to \mu\nu, 2.0 < \lvert\eta\rvert < 2.4$	80334.1	34.5	110.1	0.0	2.5	6.4	6.7	6.0	31.8	120.2
$W^- \to \mu\nu, \lvert\eta\rvert < 0.8$	80427.8	23.3	11.6	0.0	2.6	5.8	8.1	6.0	26.4	39.0
$W^- \to \mu\nu, 0.8 < \lvert\eta\rvert < 1.4$	80395.6	27.9	18.3	0.0	2.5	5.6	8.0	6.0	19.8	40.5
$W^- \to \mu\nu, 1.4 < \lvert\eta\rvert < 2.0$	80380.6	28.1	35.2	0.0	2.6	5.6	8.0	6.0	20.6	50.9
$W^- \to \mu\nu, 2.0 < \lvert\eta\rvert < 2.4$	80315.2	45.5	116.1	0.0	2.6	7.6	8.3	6.0	32.7	129.6
$W^+ \to e\nu, \lvert\eta\rvert < 0.6$	80336.5	22.2	0.0	20.1	2.5	6.4	9.0	5.3	24.5	40.7
$W^+ \to e\nu, 0.6 < \lvert\eta\rvert < 1.2$	80345.8	22.8	0.0	21.4	2.6	6.7	8.9	5.3	20.5	39.4
$W^+ \to e\nu, 1{,}8 < \lvert\eta\rvert < 2.4$	80344.7	24.0	0.0	30.8	2.6	11.9	6.7	5.3	24.1	48.2
$W^- \to e\nu, \lvert\eta\rvert < 0.6$	80351.0	23.1	0.0	19.8	2.6	7.2	8.1	5.3	26.6	42.2
$W^- \to e\nu, 0.6 < \lvert\eta\rvert < 1.2$	80309.8	24.9	0.0	19.7	2.7	7.3	8.0	5.3	20.9	39.9
$W^- \to e\nu, 1.8 < \lvert\eta\rvert < 2.4$	80413.4	30.1	0.0	30.7	2.7	11.5	8.3	5.3	22.7	51.0

|η| comb e → ~15 MeV
μ → ~11 MeV

Strongly correlated

Strongly correlated

|η| comb. → ~14 MeV
W+/W- comb → ~9 MeV

ATLAS 7 TeV Differential cross-section: combination

arXiv:1612.03016

- 105 measurement points: $W^{\pm}$ as function of charged lepton rapidity $|\eta^{\ell}|$, Z/γ^{*} as function of di-lepton rapidity $|y_{\ell\ell}|$ and mass $m_{\ell\ell}$
- Different detection challenges for electrons and muons
- $e-\mu$ combination to 61 final points including all correlations: $\chi^2/\mathrm{n.d.f.} = 59.5/53$

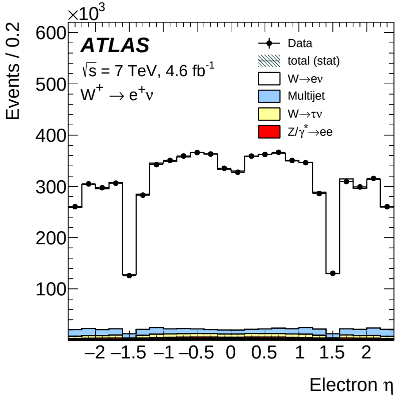

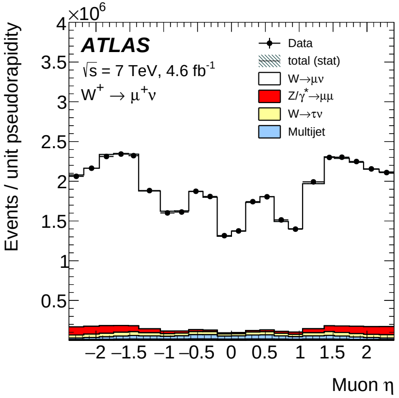

ATLAS 7 TeV Differential cross-section: combination arXiv:1612.03016

- 105 measurement points: $W^{\pm}$ as function of charged lepton rapidity $|\eta^{\ell}|$, Z/γ^{*} as function of di-lepton rapidity $|y_{\ell\ell}|$ and mass $m_{\ell\ell}$
- Different detection challenges for electrons and muons
- $e-\mu$ combination to 61 final points including all correlations: $\chi^2/\mathrm{n.d.f.} = 59.5/53$

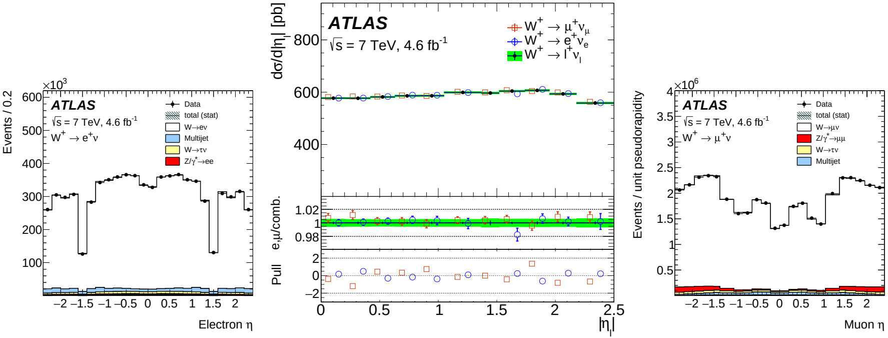

ATLAS 7 TeV Differential cross-section: combination

arXiv:1612.03016

- 105 measurement points: $W^{\pm}$ as function of charged lepton rapidity $|\eta^{\ell}|$, Z/γ^{*} as function of di-lepton rapidity $|y_{\ell\ell}|$ and mass $m_{\ell\ell}$
- Different detection challenges for electrons and muons
- $e-\mu$ combination to 61 final points including all correlations: $\chi^2/\mathrm{n.d.f.} = 59.5/53$